Medical Mycology, 2016, 54, 699–713
doi: 10.1093/mmy/myw025
Advance Access Publication Date: 9 May 2016
Original Article

Original Article

Cutaneous hyalohyphomycosis due to *Parengyodontium album* gen. et comb. nov.

Chi-Ching Tsang[1], Jasper F. W. Chan[1,2,3,4], Wai-Mei Pong[5], Jonathan H. K. Chen[1], Antonio H. Y. Ngan[1], Mei Cheung[1,5], Christopher K. C. Lai[5], Dominic N. C. Tsang[5], Susanna K. P. Lau[1,2,3,4,6,*] and Patrick C. Y. Woo[1,2,3,4,6,*]

[1]Department of Microbiology, [2]State Key Laboratory of Emerging Infectious Diseases, [3]Research Centre of Infection and Immunology, [4]Carol Yu Centre for Infection, the University of Hong Kong, Hong Kong, [5]Department of Pathology, Queen Elizabeth Hospital, Hong Kong and [6]Collaborative Innovation Center for Diagnosis and Treatment of Infectious Diseases, Zhejiang University, Hangzhou, China

*To whom correspondence should be addressed. Susanna K. P. Lau and Patrick C. Y. Woo, Department of Microbiology, the University of Hong Kong. 4/F, University Pathology Building, Queen Mary Hospital, Hong Kong. Tel: +852-2255-4892. Fax: +852-2855-1241; E-mail: pcywoo@hku.hk; and skplau@hku.hk

Received 24 November 2015; Revised 29 February 2016; Accepted 10 March 2016

Abstract

"*Engyodontium album*" is an environmental saprobic mould and an emerging opportunistic pathogen able to cause both superficial and systemic infections. In this study, we isolated a mould from the skin lesion biopsy specimen of the right shin in a patient who received renal transplantation for end-stage renal failure with prednisolone, tacrolimus, and azathioprine immunosuppressant therapy. Histology of the skin biopsy showed mild squamous hyperplasia and neutrophilic infiltrate in the epidermis, active chronic inflammation in the dermis, and fat necrosis in the subcutis, with numerous fungal elements within the serum crusts. On Sabouraud glucose agar, the fungus grew as white, cobweb-like, floccose colonies. Microscopically, conidiogenous cells were arranged in whorls of one to seven at wide angles, with zigzag-shaped terminal fertile regions and smooth, hyaline, oval, apiculate conidia. DNA sequencing showed the mould isolate belonged to "*E. album*" but matrix-assisted laser desorption ionisation–time of flight mass spectrometry (MALDI-TOF MS) failed to identify the isolate. Phylogenetic analyses based on the internal transcribed spacer region, 28S nuclear ribosomal DNA, and β-tubulin gene and MALDI-TOF MS coupled with hierarchical cluster analysis showed that "*E. album*" is distantly related to other *Engyodontium* species and should be transferred to a novel genus within the family *Cordycipitaceae*, for which the name *Parengyodontium album* gen. et comb. nov. is proposed. Three potential cryptic species within this species complex were also revealed. Antifungal susceptibility testing showed posaconazole and voriconazole had high activities against all clinical *P. album* isolates and may be better drug options for treating *P. album* infections.

Key words: *Parengyodontium*, *Parengyodontium album*, *Engyodontium album*, cutaneous hyalohyphomycosis, cryptic species, *Cordycipitaceae*.

Introduction

The genus *Engyodontium* was established in 1972 to accommodate fungi that form white, cottony, cobweb-like colonies with subverticillate to verticillate conidiophores and produce small, hyaline, and one-celled conidia.[1] Members of this genus are considered to display features intermediate between *Verticillium* and *Aphanocladium*.[2] After several taxonomical changes, *Engyodontium* currently contains four species, namely, *E. parvisporum* (type species), *E. album*, *E. geniculatum*, and *E. rectidentatum*.[2,3] Two of them, *E. parvisporum* and *E. geniculatum*, tend to have an affinity to arthropod hosts.[2] On the other hand, being the most commonly encountered species among all the four members of *Engyodontium*, *E. album* is an environmental saprobe and it can be isolated from marine sediments,[4–6] plant materials,[7] soil,[8] and walls/paintings.[9,10]

One important feature of *E. album* is its ability to produce different kinds of proteases,[5,11] and this characteristic of the fungus has long been utilized in the biotechnology industry for the mass production of proteinase K. The proteolytic and keratinolytic activities of *E. album* make it an opportunistic human pathogen.[10,12] Moreover, *E. album* is able to produce cytotoxic polyketides, which have been demonstrated to inhibit vascular endothelial cell growth factor (VEGF) signalling and exhibit cytotoxicity against human histiocytic lymphoma cell line U937.[6,13] This further demonstrated the pathogenicity of *E. album*. Infections caused by *E. album* in human are emerging and include breast granulomatosis,[14,15] cerebritis,[15] eczema vesiculosum,[16] endocarditis,[17,18] fungaemia,[12] and keratitis.[19,20] Recently, it was also reported that *E. album* could cause fatal infections in spiders.[21]

In 2012, we isolated a mould from the biopsy specimen of a crusted skin lesion at the right shin of a patient. Microscopic examination of the fungal culture and internal transcribed spacer (ITS) sequencing showed that it should belong to *E. album*. However, further genotypic and matrix-assisted laser desorption ionisation–time of flight mass spectrometry (MALDI-TOF MS) analyses of the fungal isolate, additional *E. album* reference strains and other *Engyodontium* species suggested that *E. album* is phylogenetically and chemotaxonomically distinct from other members of *Engyodontium*. Therefore, we propose to transfer this fungal species to the novel genus, *Parengyodontium* gen. nov., with the new name *Parengyodontium album* comb. nov. describing this fungus. Its characterizations also revealed that the *P. album* species complex may actually contain three different cryptic species.

Materials and methods

Patient and strains

Clinical specimens were collected and handled according to standard protocols, and were cultured on Sabouraud glucose agar (SGA) (Oxoid, UK) supplemented with chloramphenicol (50 μg/ml) (Sigma-Aldrich, St. Louis, MO, USA) at 30 °C to obtain the case isolate HKU48. Clinical data were collected by retrieving and analysing the hospital record of the patient. Thirteen other *E. album* reference strains, ten of which from human/veterinary origins, were obtained from the Agricultural Research Service (ARS) Culture Collection (NRRL), Department of Agriculture, USA; Centraalbureau voor Schimmelcultures of the Royal Netherlands Academy of Arts and Sciences (CBS-KNAW Fungal Biodiversity Centre), the Netherlands; Mycology Laboratory of the Institute of Hygiene and Epidemiology (IHEM), Belgian Coordinated Collections of Microorganisms (BCCM), Belgium; and University of Alberta Microfungus Collection and Herbarium (UAMH), Canada. In addition, reference strains of other *Engyodontium* or closely related species were obtained from CBS and IHEM (Table 1). The reference strains *Issatchenkia orientalis* (synonym: *Candida krusei*) ATCC 6258^T and *C. parapsilosis* ATCC 22019^T were obtained from the American Type Culture Collection (ATCC), USA.

Phenotypic characterisations

The fungal isolate HKU48 and other reference strains were cultured on Czapek's agar (CZA) (homemade),[22] malt extract agar (MEA) (Oxoid), potato dextrose agar (PDA) (BD Diagnostic Systems, Sparks, MD, USA), and SGA [all supplemented with chloramphenicol (50 μg/ml)] for examination of colony characteristics. Microscopic characteristics were observed for cultures grown on home-made tap water agar by both direct examination of the agar plates and the agar block smear preparation method.[23] HKU48 was also microscopically examined by scanning electron microscopy (SEM), performed according to our previous publication.[24]

Table 1. Information of fungal strains characterized in this study.

Species	Strain[a]	Isolation source	ITS	28S nrDNA	β-tubulin
Parengyodontium album comb. nov.					
Subclade 1	HKU48	Human skin biopsy	LC092879	LC092898	LC092917
	CBS 504.83^{ET}	Human brain abscess	LC092880	LC092899	LC092918
	CBS 570.71	Human	LC092881	LC092900	LC092919
	CBS 836.71	Pea	LC092882	LC092901	LC092920
	CBS 121919	Uncontrolled diabetic patient with conjunctivitis	LC092883	LC092902	LC092921
	UAMH 1441	Human skin	LC092884	LC092903	LC092922
	UAMH 10043	Broodmare pleural fluid	LC092885	LC092904	LC092923
	NRRL 2312	Soil	LC092886	LC092905	LC092924
Subclade 2	IHEM 4198	Human ear secretions	LC092887	LC092906	LC092925
	UAMH 4512	Human eye wound	LC092888	LC092907	LC092926
	UAMH 8313	Human blood	LC092889	LC092908	LC092927
	UAMH 11234	Human bioprostheric valve	LC092890	LC092909	LC092928
Subclade 3	CBS 368.72	Fresco	LC092891	LC092910	LC092929
	UAMH 9836	Human bronchoscopy specimen	LC092892	LC092911	LC092930
Engyodontium rectidentatum	CBS 206.74	Air	LC092893	LC092912	LC092931
	CBS 547.82	N/A[b]	LC092894	LC092913	LC092932
	CBS 641.74	Buried keratinous substance	LC092895	LC092914	
Engyodontium parvisporum	IHEM 22910	Indoor contamination	LC092896	LC092915	LC092933
Lecanicillium tenuipes	CBS 658.80	Spider	LC092897	LC092916	LC092934

[a]CBS, Centraalbureau voor Schimmelcultures of the Royal Netherlands Academy of Arts and Sciences, the Netherlands; HKU, the University of Hong Kong, Hong Kong; IHEM, Mycology Laboratory of the Institute of Hygiene and Epidemiology, Belgian Coordinated Collections of Microorganisms, Belgium; NRRL, Agricultural Research Service Culture Collection, Department of Agriculture, the United States of America; UAMH, the University of Alberta Microfungus Collection and Herbarium, Canada.
[b]N/A, not available.

DNA extraction, ITS, partial 28S nrDNA, and partial β-tubulin gene sequencing, sequence identity analyses and phylogenetic analyses

Extraction of fungal DNA, polymerase chain reaction (PCR), and sequencing of the ITS, partial 28S nuclear ribosomal DNA (nrDNA), and partial β-tubulin gene for the case isolate HKU48 and the reference strains were carried out following our previous publication[25] with the primer pairs ITS1[26] and ITS4[26] (ITS), NL1[27] and NL4[27] (28S nrDNA), as well as Bt2a[28] and Bt2b[28] (β-tubulin gene). The DNA sequences obtained, together with those of other closely related species accessioned in the DDBJ/ENA/GenBank databases, were then compared by pairwise alignment using BioEdit 7.2.0.[29] These sequences were also analysed by multiple sequence alignment using MUSCLE 3.8.[30] After end-trimming, divergent or poorly aligned regions of the DNA sequences were removed using Gblocks 0.91b[31,32] with relaxed parameters. Tests for substitution models and phylogenetic tree construction were performed by the maximum likelihood method using MEGA 6.0.6.[33] Phylogenetic analyses at the *Cordycipitaceae* family level[34] included 347 and 404 nucleotide positions of the ITS and partial 28S nrDNA, respectively; while phylogenetic analyses at the "*E. album*" isolates level included 416, 458, and 314 nucleotide positions of the ITS, partial 28S nrDNA, and partial β-tubulin gene, respectively. A phylogenetic tree was also constructed using the concatenated sequences of the ITS, partial 28S nrDNA, and partial β-tubulin gene (1,410 nucleotide positions) of the "*E. album*" isolates and other closely related strains.

MALDI-TOF MS

MALDI-TOF MS was performed using the microflex LT system (Bruker Daltonics, Germany) by the formic acid extraction method according to the manufacturer's instruction and our previous publication.[24] The Filamentous Fungi Library v1.0 (Bruker Daltonics) database was used for fungal identification. Furthermore, for each fungal strain the mass spectra produced were processed and integrated

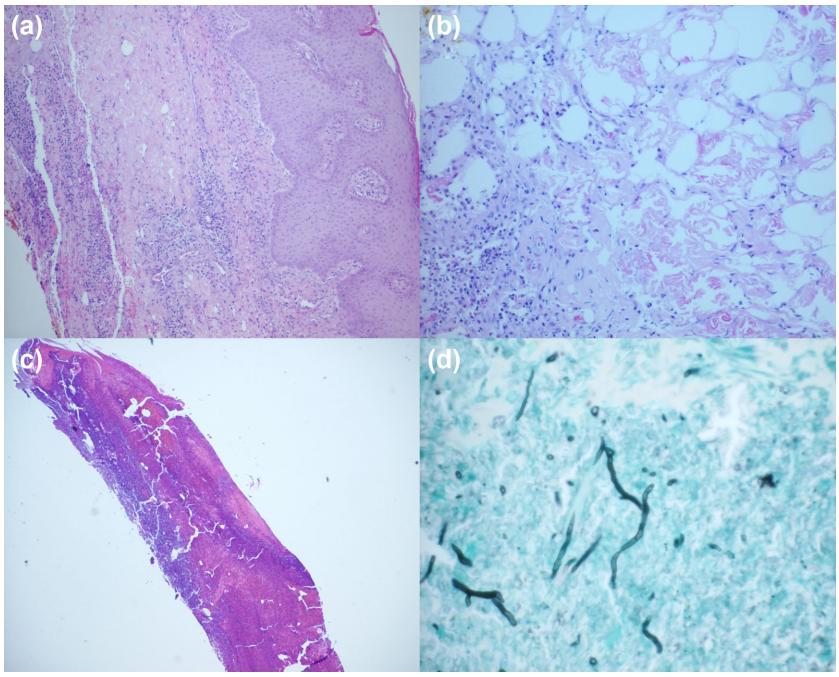

Figure 1. Photomicrographs of the biopsied right shin skin lesion. (a) Mild squamous hyperplasia and neutrophilic infiltrate in the epidermis with active chronic inflammation in the dermis (hematoxylin-eosin stain, original magnification 200×). (b) Fat necrosis associated with neutrophilic infiltrate in the subcutis (hematoxylin-eosin stain, original magnification 400×). (c) Serum crusts enmeshing degenerated inflammatory cells (hematoxylin-eosin stain, original magnification 40×). (d) Numerous septate fungal hyphae within the serum crusts (Grocott's methenamine silver stain, original magnification 400×).

to generate a mass spectrum profile (MSP) using MALDI Biotyper 3.1 (Bruker Daltonics), and the MSPs of all the strains were then characterised by hierarchical cluster analysis (HCA) to generate a dendrogram using MALDI Biotyper 3.1.

Antifungal susceptibility test

The *in vitro* susceptibilities of *E. album* strains of clinical origins to nine different antifungal drugs were tested using the Sensititre YeastOne plates (Trek Diagnostic Systems, UK) according to the manufacturer's protocol for *Aspergillus* species and our previous publication.[35] The plates were incubated at 30 °C or 35 °C, and the results were recorded after 72 hours of incubation, except that the results for IHEM 4198 and UAMH 8313 were read after 96 hours of incubation due to their slow growth at 35 °C. The reference strains *I. orientalis* ATCC 6258^T and *C. parapsilosis* ATCC 22019^T were used as quality controls.

Data availability

The ITS, partial 28S nrDNA, and partial β-tubulin gene sequences of HKU48 and the reference strains have been deposited in the DDBJ/ENA/GenBank databases with the accession numbers LC092879-LC092934 (Table 1). The ITS sequences of HKU48 and the reference strains were also deposited in the International Society for Human and Animal Mycology (ISHAM) ITS Database[36] (freely available at http://its.mycologylab.org/) with the sequence unique identifiers MITS3582-MITS3600. The MALDI-TOF MSPs of HKU48 and the reference strains have been deposited in the Spectra database, the Public Health Agency of Sweden (Folkhälsomyndigheten) (freely available at http://spectra.folkhalsomyndigheten.se/spectra/).

Results

Patient

A 60-year-old Chinese man complained of a crusted skin lesion over the right shin that has lasted for two months prior to the present admission for management of nontyphoidal *Salmonella* mycotic aneurysm at the infra-renal abdominal aorta. The patient had undergone renal transplantation for end-stage renal failure 10 years prior to admission and was on multiple maintenance immunosuppressants including prednisolone, tacrolimus, and azathioprine. His other infective complications after the renal transplantation included recurrent urinary tract infections, cytomegalovirus reactivation, and herpes zoster. Physical examination

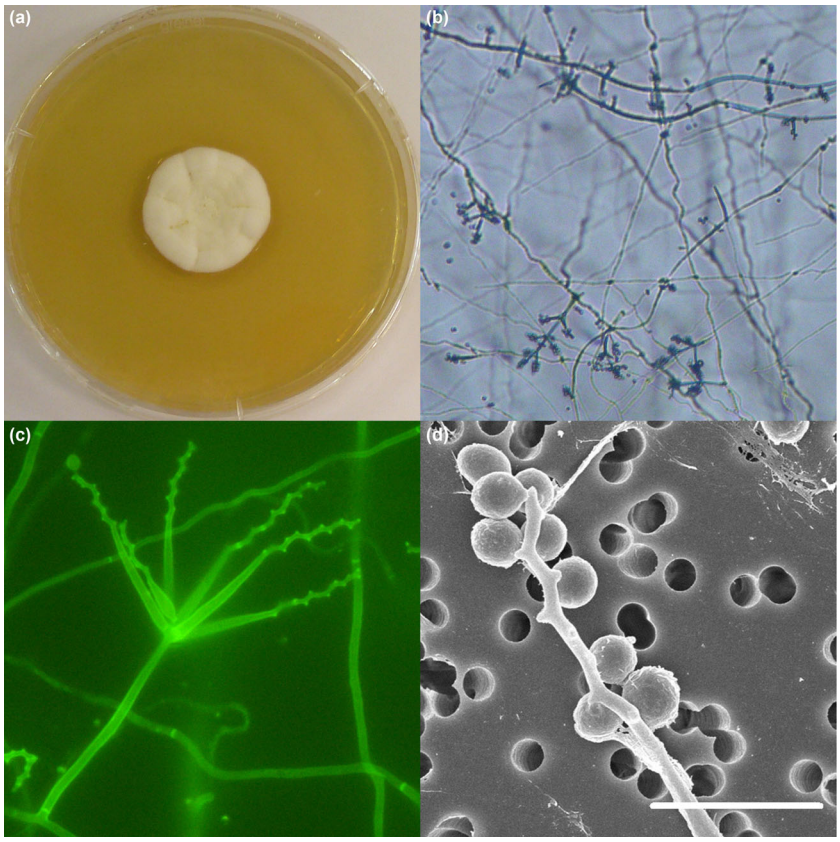

Figure 2. Macro- and microscopic morphology of *Parengyodontium album*. (a) Colony surface of HKU48 on SGA after 14 d of incubation at 25 °C. (b) Conidiogenous cells arranged in whorls of smooth-walled conidiophores (direct examination, original magnification 100×). (c) Whorl of conidiogenous cells (mounted with 5% KOH and calcofluor white stain, original magnification 1,000×). (d) Conidia smooth, hyaline, oval, apiculate, and produced at each bent point of the zigzag rachides. (SEM, scale bar = 5 μm).

revealed a 5 cm × 4 cm × 3.5 cm, crusted, nontender lesion with overlying inflammatory skin changes at the right shin. There was no bleeding or ulceration. Laboratory tests showed leukopenia (2.9 × 10^9/l; reference range: 3.7–9.2 × 10^9/l) with marked lymphopenia (0.1 × 10^9/l; reference range: 1.0–3.1 × 10^9/l), hypoalbuminaemia (24 g/l; reference range: 35–52 mmol/l), and normal liver function tests and serum creatinine levels. Biopsy of the lesion showed mild squamous hyperplasia and neutrophilic infiltrate in the epidermis and active chronic inflammation in the dermis (Fig. 1a), fat necrosis associated with neutrophilic infiltrate in the subcutis (Fig. 1b), and serum crusts enmeshing degenerated inflammatory cells (Fig. 1c). Numerous septate fungal hyphae were identified within the serum crusts in the Grocott's methenamine silver-stained section (Fig. 1d). Gram and Ziehl-Neelsen stains did not show any bacteria or acid-fast bacilli. Culture of the biopsied tissue and skin swab revealed tiny, white, cottony mould colonies at the primary inoculation sites after three days of incubation at 30 °C on SGA supplemented with chloramphenicol. The fungal isolate (HKU48) was cryopreserved at −80 °C for further characterisation, and it was also deposited into the Biological Resource Center, National Institute of Technology and Evaluation (NBRC), Japan, with the accession number NBRC 111624; as well as the National Collection of Pathogenic Fungi (NCPF), Public Health England (PHE) Mycology Reference Laboratory, UK, with the accession number NCPF 7880. No bacteria or mycobacteria were isolated. The patient was treated with oral itraconazole 200 mg twice daily. However, he developed nosocomial pneumonia with acute respiratory failure after prolonged hospitalisation. He succumbed two months after hospitalisation.

Phenotypic characterisations

The colonies of HKU48 on CZA, MEA, PDA, and SGA were similar in morphology and were white, cobweb-like, floccose, and velvety to downy, with radial folding. No diffusing pigment was observed on all these culture media (Fig. 2a). Microscopically, hyphae were septate. Conidiophores were smooth-walled and possessed many verticillate side branches, having conidiogenous cells arranged in whorls of one to seven at wide angles which were occasionally biverticillate (Fig. 2b). Each conidiogenous cell had an

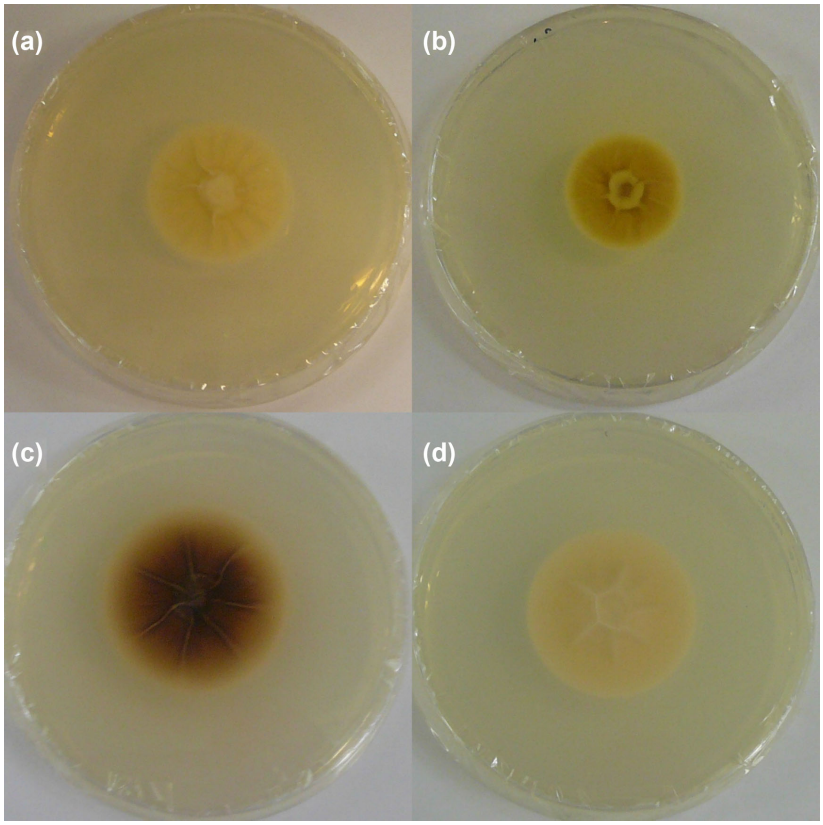

Figure 3. Colony reverses of different *Parengyodontium album* strains on PDA after 14 d of incubation at 25 °C exhibiting different colours. (a) Strain HKU48 (white). (b) Strain CBS 504.83^{ET} (subclade 1, orange-brown). (c) Strain UAMH 8313 (subclade 2, dark brown). (d) Strain CBS 368.72 (subclade 3, white).

elongated basal part, which tapered toward the tip with a zigzag rachis (Fig. 2c). Smooth, hyaline, oval, and apiculate conidia were produced at each bent point of the zigzag rachises (Fig. 2d). No growth was observed at temperatures at or above 32 °C.

Among HKU48 and other *E. album* reference strains, different colours of colony reverses were observed when cultured on PDA. The colony reverses on PDA of strains HKU48, CBS 368.72, and UAMH 9836 were white; those of strains CBS 504.83^{ET}, CBS 570.71, CBS 836.71, CBS 121919, UAMH 1441, UAMH 10043, and NRRL 2312 were orange-brown (intermediate); while those of strains IHEM 4198, UAMH 4512, UAMH 8313, and UAMH 11234 were dark brown in colour (Fig. 3). Such intra-species colour variation of colony reverses was not observed on the other culture media used.

ITS, partial 28S nrDNA and partial β-tubulin gene sequencing, sequence identity analyses and phylogenetic analyses

PCR of the ITS, partial 28S nrDNA, and partial β-tubulin gene of HKU48 and the reference strains yielded DNA products with lengths of about 550 bp, 550 bp, and 300 bp, respectively. Pairwise alignment showed the ITS sequence of HKU48 possessed 96.0–100% sequence identities to other *E. album* strains, but only 88.1–88.8% sequence identities to other *Engyodontium* species; the partial 28S nrDNA sequence of HKU48 possessed 99.3–100% sequence identities to other *E. album* strains, but only 96.7–96.9% sequence identities to other *Engyodontium* species; and the partial β-tubulin gene sequence of HKU48 possessed 93.6–100% sequence identities to other *E. album* strains, but only 83.4–85.6% sequence identities to other *Engyodontium* species. Phylogenetic analyses based on the ITS and partial 28S nrDNA showed that HKU48 was grouped into a highly supported cluster together with other *E. album* strains (Fig. 4). This *E. album* cluster was the most closely related to *Lecanicillium kalimantanense* and *L. wallacei*, but it was also shown to be distinctly related to other *Engyodontium* species phylogenetically (Fig. 4), suggesting that *E. album* should be transferred to a novel genus in the family *Cordycipitaceae*. Moreover, phylogenetic analyses based on the ITS, partial 28S nrDNA, and partial β-tubulin gene showed that although all the *E. album* strains were grouped in a single monophyletic cluster, they were separated into three distinct subclades (Fig. 5 and Suppl. Fig. S1).

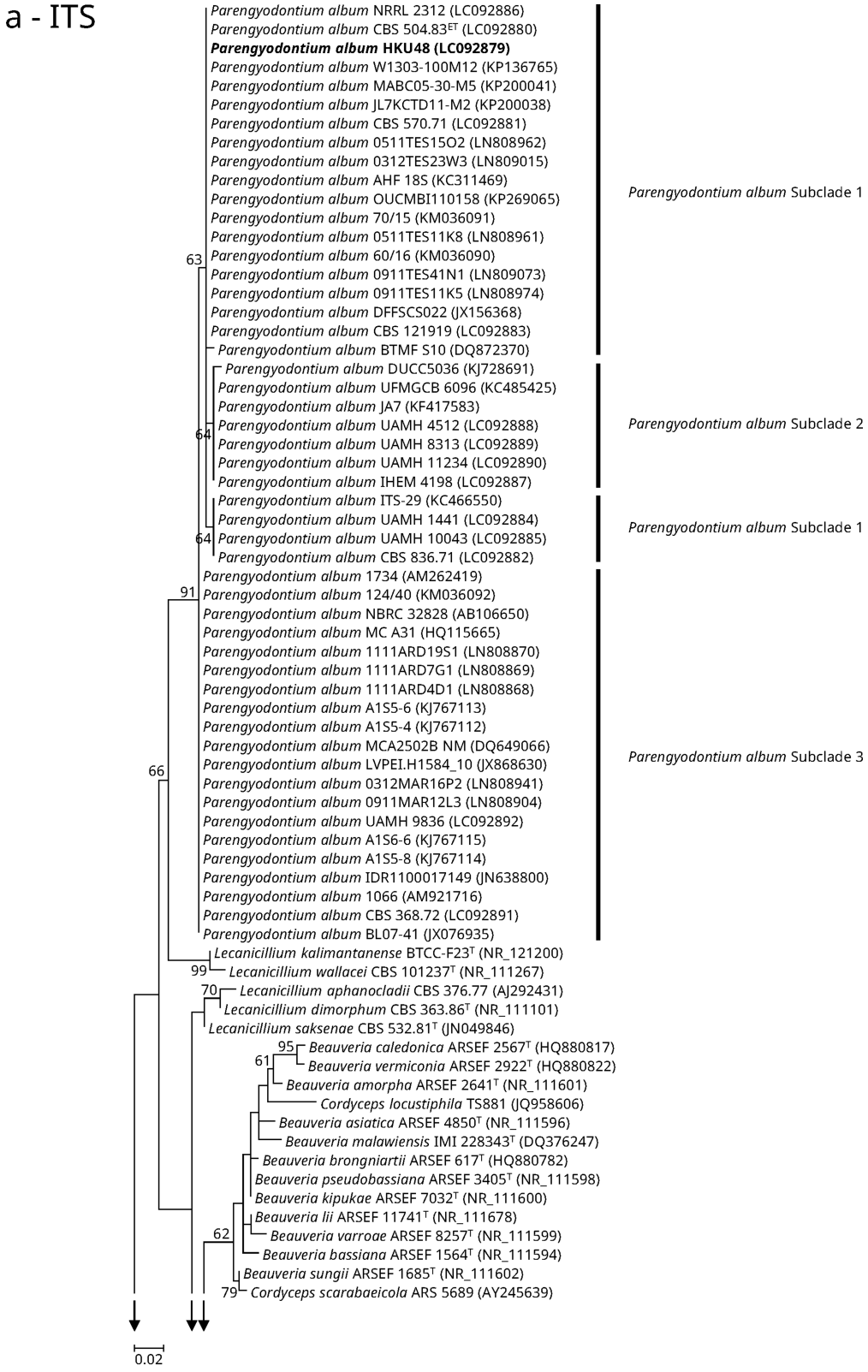

Figure 4. Phylogenetic trees showing the relationship of *Parengyodontium album* to its closely related species of the family *Cordycipitaceae*.[34] The trees were inferred from (a) ITS and (b) partial 28S nrDNA sequence data by the maximum likelihood method with the substitution models K2 (Kimura 2-parameter model) + G (gamma-distributed rate variation) + I (estimated proportion of invariable sites) and T92 (Tamura 3-parameter model) + G + I, respectively. The scale bars indicate the estimated numbers of substitutions per base. Numbers at nodes indicate levels of bootstrap support calculated from 1,000 replicates, and values lower than 60 are not shown. All names and accession numbers are given as cited in the DDBJ/ENA/GenBank databases.

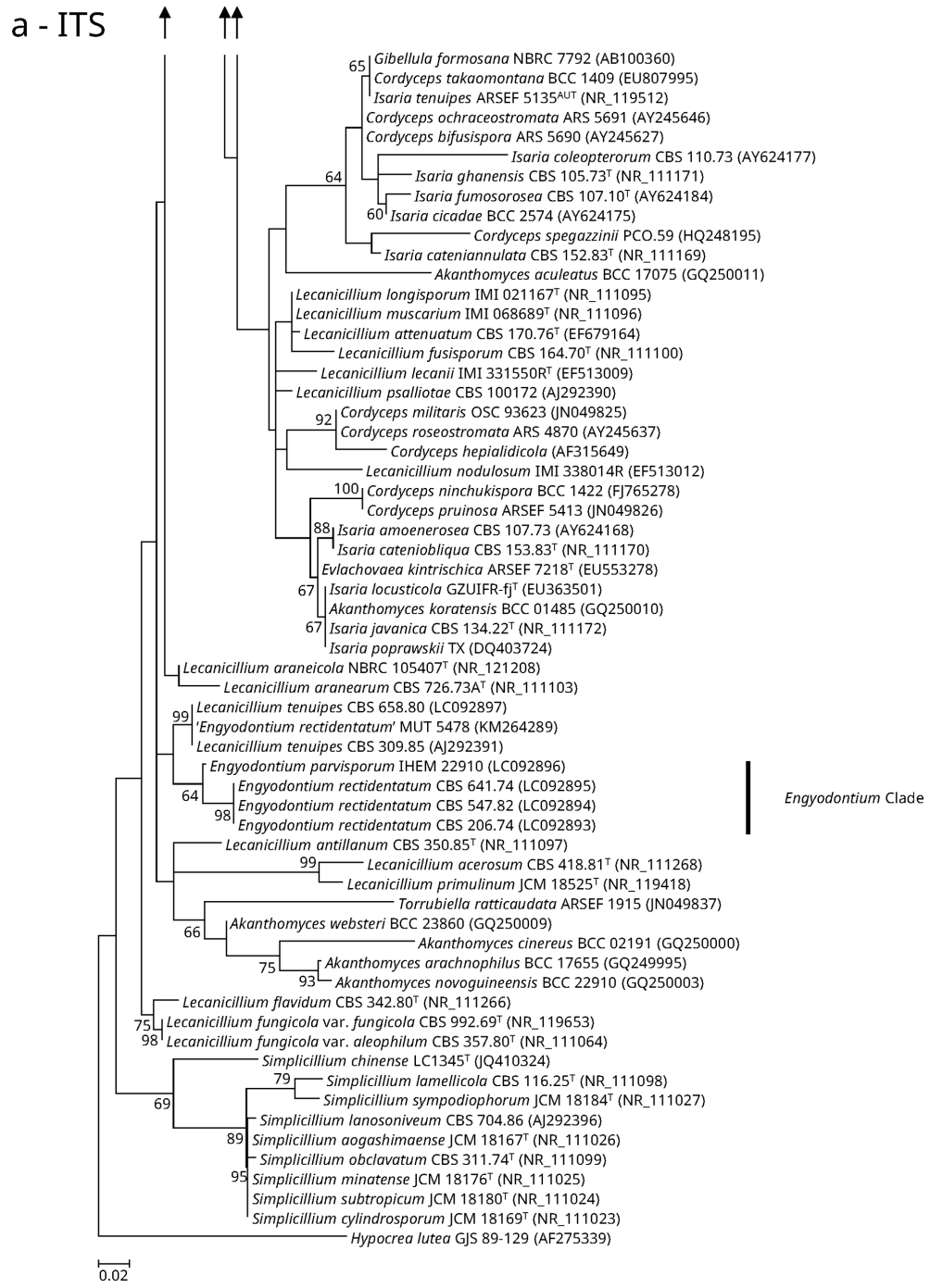

Figure 4. *Continued.*

MALDI-TOF MS

None of the fungal strains characterised in this study (HKU48, additional *E. album* reference strains, and other *Engyodontium* species) could be identified by MALDI-TOF MS, which was probably due to a lack of their reference protein mass spectra in the Bruker Daltonics Filamentous Fungi Library v1.0 MS database. HCA of the protein mass spectra of HKU48, additional *E. album* reference strains, and other *Engyodontium* species showed that all the *E. album* strains characterised were grouped separately from other *Engyodontium* species (Fig. 6). Within the *E. album* cluster all the strains were grouped into three distinct subclades which corresponded to those observed in the phylogenetic trees (Fig. 6).

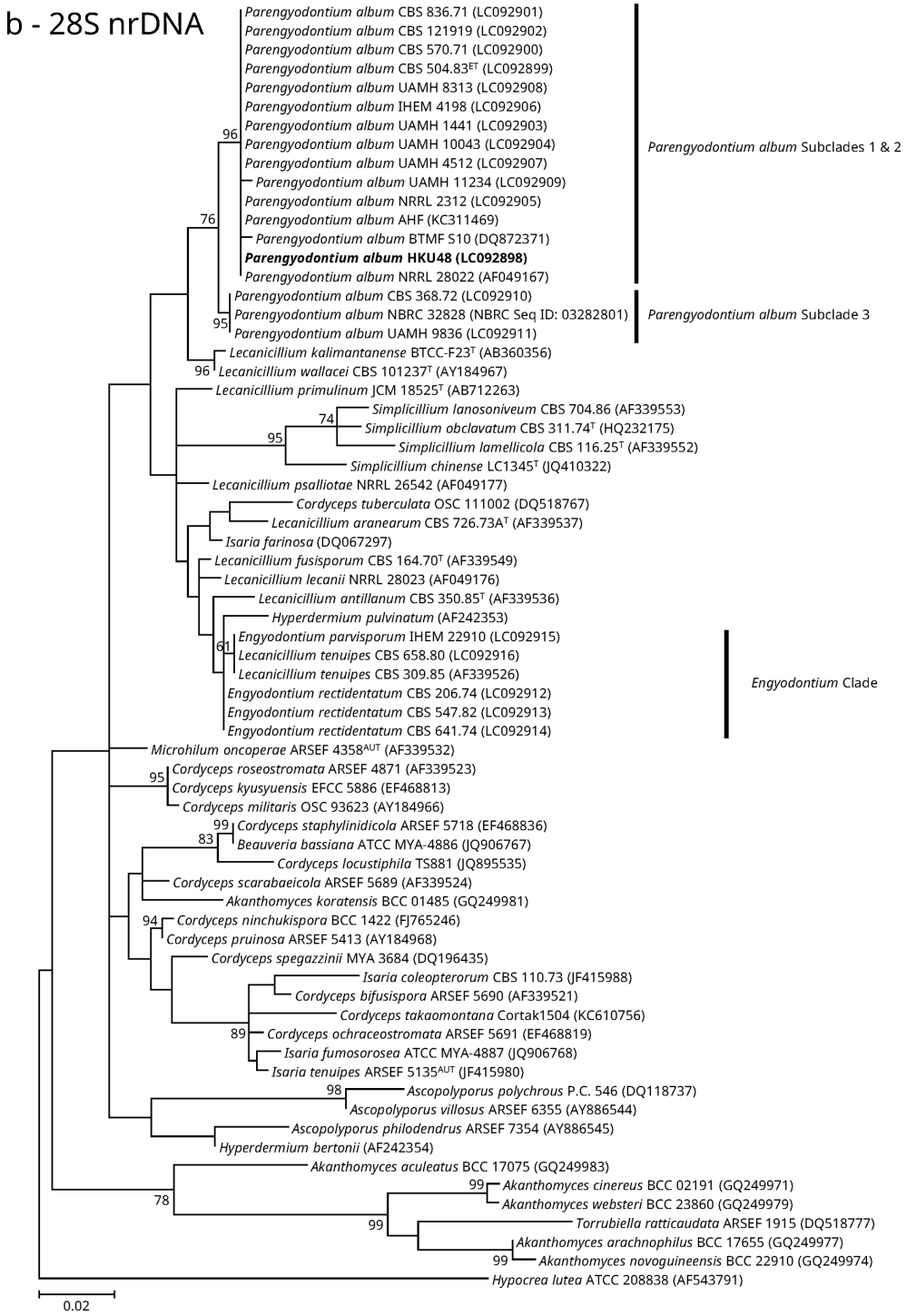

Figure 4. *Continued.*

Antifungal susceptibilities of clinical *E. album* strains

The *in vitro* susceptibilities of the clinical *E. album* strains to nine different antifungal agents are listed in Table 2. All of the clinical strains have high MICs to flucytosine and fluconazole, and most clinical strains have low MICs to posaconazole and voriconazole. Most clinical strains of subclade 1 of *E. album* have high MICs to itraconazole. In the contrary, all clinical strains of subclades 2 and 3 of *E. album* have low MICs to itraconazole.

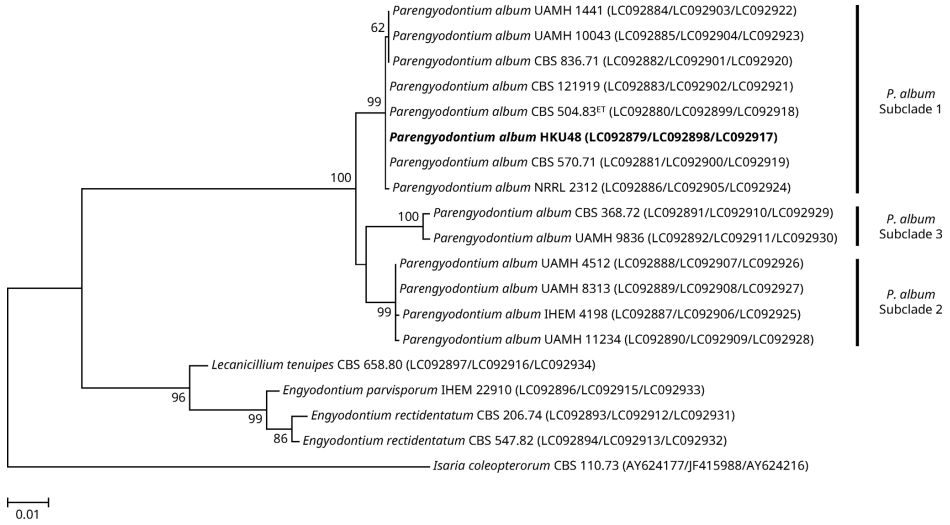

Figure 5. Phylogenetic tree showing the relationship of *Parengyodontium album* to *Engyodontium* and other closely related species. The tree was inferred from the concatenated ITS, partial 28S nrDNA, and partial β-tubulin sequence data by the maximum likelihood method with the substitution model TN93 (Tamura-Nei model) + G. The scale bar indicates the estimated number of substitutions per base. Numbers at nodes indicate levels of bootstrap support calculated from 1,000 trees and bootstrap values lower than 60 are not shown. All names and accession numbers are given as cited in the DDBJ/ENA/GenBank databases.

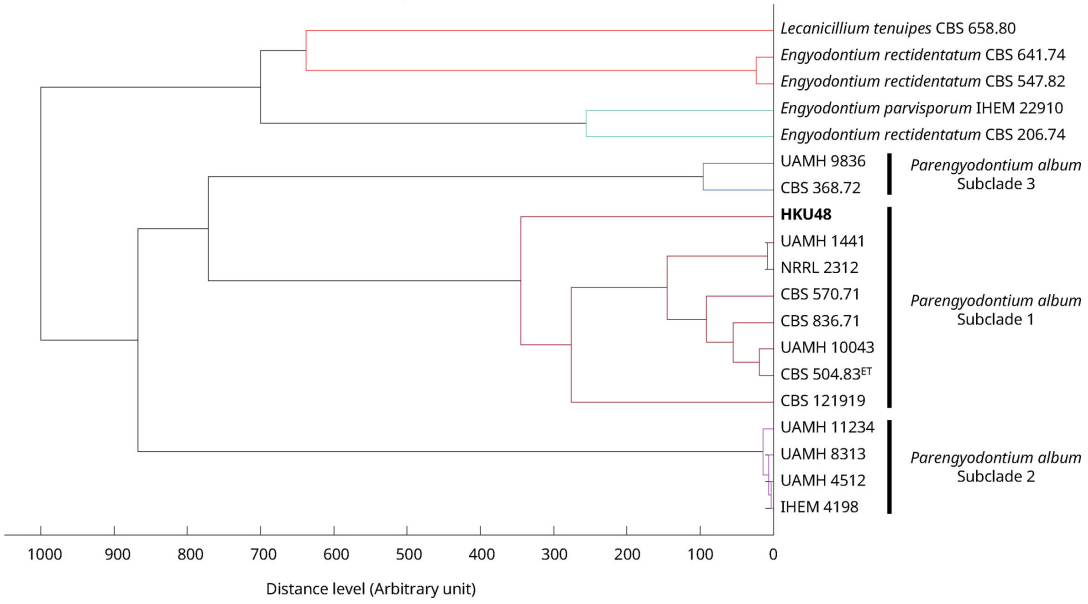

Figure 6. Dendrogram generated from hierarchical cluster analysis of MALDI-TOF mass spectra of *Parengyodontium album*, *Engyodontium* species, and related species.

Taxonomy

Parengyodontium C.-C. Tsang, J.F.W. Chan, W.-M. Pong, J.H.K. Chen, A.H.Y. Ngan, M. Cheung, C.K.C. Lai, D.N.C. Tsang, S.K.P. Lau, P.C.Y. Woo, gen. nov.

Mycobank accession number: MB 815049. Type species: *Parengyodontium album*. Etymology: name refers to the *Engyodontium*-like morphology of this group of fungi.

Colonies white, cobweb-like, lanose to floccose, velvety to downy, without diffusing pigment. Hyphae septate. Conidiophores erect or procumbent, bearing numerous whorls of conidiogenous cells. Basal part of conidiogenous cells elongated and tapering, and terminal fertile region zigzag in shape. Conidia smooth, hyaline, globose to subglobose, apiculate, and produced at each bent point of the zigzag rachides.

Table 2. Minimum inhibitory concentrations of different antifungal agents against clinical *Parengyodontium album* isolates.

Subclade (Incubation temperature)	Strain	MICs (μg/ml)								
		AND	CAS	MF	FC	FZ	IZ	PZ	VO	AB
Subclade 1 (30 °C)	HKU48	1	1	2	>64	>256	>16	0.25	0.5	2
	CBS 504.83^{ET}	0.5	0.5	4	>64	>256	>16	0.5	1	>8
	CBS 570.71	1	1	2	>64	>256	>16	0.5	2	4
	CBS 121919	2	2	4	>64	64	0.12	0.12	0.25	4
	UAMH 1441	1	1	2	>64	>256	>16	2	4	8
	UAMH 10043	2	2	8	>64	>256	>16	2	4	4
Subclade 2 (35 °C)	IHEM 4198	2	2	8	>64	32	0.25	0.12	0.06	4
	UAMH 4512	4	4	8	>64	128	0.25	0.25	0.12	2
	UAMH 8313	2	2	4	>64	8	0.03	0.03	0.03	2
	UAMH 11234	>8	8	>8	>64	128	0.25	0.06	0.06	≤0.12
Subclade 3 (30 °C)	UAMH 9836	2	2	4	>64	4	≤0.015	0.015	0.03	1

Note: AND, anidulafungin; CAS, caspofungin, MF, micafungin, FC, flucytosine; FZ, fluconazole; IZ, itraconazole; PZ, posaconazole, VO, voriconazole; AB, amphotericin B.

Parengyodontium album (Limber) C.-C. Tsang, J.F.W. Chan, W.-M. Pong, J.H.K. Chen, A.H.Y. Ngan, M. Cheung, C.K.C. Lai, D.N.C. Tsang, S.K.P. Lau, P.C.Y. Woo, comb. nov.

Mycobank accession number: MB 815050.

≡ *Tritirachium album* Limber, Mycologia 32 : 27. 1940 (basionym).

≡ *Beauveria alba* (Limber) Saccas, Revue de Mycologie 13 : 64. 1948.

≡ *Engyodontium album* (Limber) de Hoog, Persoonia 10 : 53. 1978.

The species description is emended from those given by Limber (1940),[37] de Hoog (1972),[16] Matsushima (1975),[38] de Hoog (1978),[1] and de Hoog et al (2000).[39] Colonies white, cobweb-like, lanose to floccose, velvety to downy, without diffusing pigment. On PDA, colony reverse white to orange-brown to dark brown in colour. Hyphae septate. Conidiophores erect or procumbent, occasionally biverticillate, bearing numerous (one to seven) whorls of conidiogenous cells at wide, often right, angles. Basal part of conidiogenous cells elongated and tapering (10–24 × 1.5–2.5 μm), and terminal fertile region zigzag in shape. Whole conidiogenous cell up to 35 μm long. Conidia smooth, hyaline, globose to subglobose (1.1–2.5 × 1.4–3.2 μm), apiculate, and produced at each bent point of the zigzag rachides.

Holotype: BPI 414591, from cover of book, Woods Hole, MA, USA; the specimen is historical and no ex-type culture or DNA material is available (not examined in this study). Epitype designated here that supports the holotype cited above: CBS H-22418 (MBT 203989), from human brain abscess, Germany. Ex-epitype culture: CBS 504.83^{ET} (= ATCC 56482^{ET}). Other materials examined: HKU48 (= NBRC 111624 = NCPF 7880), from the biopsy specimen of a crusted skin lesion at the right shin of a human, Hong Kong; CBS 368.72, from fresco, Romania; CBS 570.71, from human, the Netherlands; CBS 836.71, from *Pisum sativum* (pea), Israel; CBS 121919, from an uncontrolled diabetic patient with conjunctivitis, India; IHEM 4198, from human ear secretions, Italy; NRRL 2312, from dismal swamp soil, USA; UAMH 1441, from human skin, the Netherlands; UAMH 4512, from a human eye wound, USA; UAMH 8313, from human blood, Canada; UAMH 9836, from a human bronchoscopy specimen, Canada; UAMH 10043, from broodmare pleural fluid, USA; UAMH 11234, from human bioprosthetic valve, USA.

Parengyodontium represents a distinct phylogenetic lineage within the family *Cordycipitaceae*. At the present time this genus only accommodates one single species, *P. album*. *Parengyodontium* differs from the phylogenetically most closely related species *L. kalimantanense* and *L. wallacei* by having zigzag-shaped ends of conidiogenous cells, and globose to subglobose, apiculate conidia. *Parengyodontium* also differs from *Engyodontium* phylogenetically and chemotaxonomically. Given the historical nature of the holotype specimen and the unavailability of ex-holotype culture or holotypic DNA material, the designation of an epitype for this species is necessary. The strain CBS 504.83^{ET}, belonging to subclade 1, exhibited features which closely resembled the cultural characters of the holotype of *P. album* as described by Limber,[37] and is therefore designated here as the ex-epitype of this species.

Discussion

We report the recovery of the isolate HKU48 in pure culture from the biopsied specimen of a crusted skin lesion at the right shin of a patient. The clinical importance of the fungus was demonstrated by the invasion of the fungus into the skin tissue of the patient and also the inflammatory responses in the biopsied specimen as observed under histological examination. In addition, mycological culture of the biopsied specimen yielded fungal colonies at the primary inoculation sites on all agar plates, which supported that the isolate was originated from the clinical specimen, rather than being a mere contaminant. Although there have only been six reported cases of *E. album* infection in humans, infectious diseases due to *E. album* are emerging, with more than half of these cases reported within the past ten years (Table 3).[12,14,15,17–20] Among the six reported cases, two patients died of *E. album* infection, one with brain abscess,[15] and the other with infective endocarditis.[17]

Molecular characterisation suggested a new taxonomic position for *E. album*. Sequencing and phylogenetic analyses based on three different DNA regions showed that HKU48 belonged to "*E. album*" (Figs. 4 and 5, Suppl. Fig. S1). Although "*E. album*" was classified in the genus *Engyodontium* based on morphological characterization, it formed a distinct phylogenetic lineage from other members of *Engyodontium*, being most closely related to *L. kalimantanense* and *L. wallacei* (Fig. 4). Phylogenetic analyses also showed that the genus *Lecanicillium* is polyphyletic, and the type species of this genus, *L. lecanii*, is distantly related to "*E. album*", *L. kalimantanense*, and *L. wallacei* (Fig. 4). This suggested that "*E. album*" should be transferred to a novel genus within the family *Cordycipitaceae*, for which the name *Parengyodontium album* gen. et comb. nov. is proposed. Within the species *P. album*, cryptic species may also exist. In the phylogenetic trees inferred from the ITS, partial 28S nrDNA, and partial β-tubulin gene sequence data, different strains of *P. album* were grouped into three different subclades (Fig. 5 and Suppl. Fig. S1). Similarly, this clustering could also be clearly observed in the dendrogram generated from the HCA of protein mass spectra of the *P. album* strains and related species (Fig. 6). Interestingly, it was also noted that only strains belonging to subclade 2 of *P. album* could grow at and beyond 35 °C; while those of subclades 1 and 3 did not grow beyond 31 °C. The results suggested that *P. album* may actually represent a species complex containing three cryptic species. Moreover, in general the colony reverses of the three *P. album* subclades exhibited different colours when cultured on PDA (Fig. 3). The colony reverses of most subclade 1 strains were orange-brown in colour, all subclade 2 strains were dark brown in colour, and all subclade 3 strains were white in colour. Although phylogenetic studies showed that the case isolate HKU48 belonged to subclade 1 of *P. album*, the reverse of its colony on PDA was white. Therefore, it was not sure whether the colour of colony reverse was a subclade-specific trait for *P. album*. Nevertheless, in the original species description of *P. album* (then *Tritirachium album*) by Limber the colour of substrate on PDA was said to be orange,[37] suggesting that the holotype of *P. album* may be a member of subclade 1. On the other hand, although Limber also mentioned that for the ex-holotype the colour of substrate on CZA was also orange,[37] none of the *P. album* strains characterised in this study exhibited such trait on this medium. Further characterisation is warranted to determine the subclade specificity for this colour trait of colony reverse and if it is necessary to change the ranks of the other two *P. album* subclades to species level.

Despite the fact that many *P. album* isolates (subclades 1 and 3) did not grow beyond 31 °C, the pathogenicity of *P. album* should not be underestimated. Quite a number of *P. album* isolates actually came from clinical or veterinary specimens (Table 1). Although such isolates have been questioned to be merely culture contamination rather than being the real aetiological agent, and they were shown to be avirulent using a murine model,[15] histological examination as reported by Seeliger et al.[26] and in this study showed clearly that the cultivated fungi have invaded the biopsied tissues. The absence of growth of certain fungi at 37 °C *in vitro* does not rule out their possibilities as disease-causing agents since infection may take place at the surface of the human body, where the temperature is usually lower than the core body temperature.[40] For example, *Auxarthron ostraviense* and *A. umbrinum*,[41] *Microsporum aenigmaticum*,[42] as well as *Trichophyton eboreum*,[43–45] which do not grow at 37 °C, were reported as causes of infections at superficial body sites, such as nails or the skin. This phenomenon could also be observed for *P. album*. Many clinical strains of subclades 1 and 3 of *P. album* were isolated from specimens from superficial body sites including the skin (HKU48, UAMH 1441) and the eyes (CBS 121919), while only subclade 2 of *P. album*, which could grow at or beyond 35 °C, is able to cause deep-seated infection, such as endocarditis (UAMH 11234) and fungaemia (UAMH 8313) (Table 3). Although the strain CBS 504.83^{ET} (subclade 1) was isolated from brain abscess, it belonged to subclade 1 of *P. album*, and it did not grow beyond 31 °C. A review of this case revealed that the patient first suffered from fungal granulomatous breast parenchymal lesions and subsequently due to unknown reason, the fungus somehow was able to invade the brain and caused death.[14,15]

Table 3. Infections caused by *Parengyodontium album* reported in the literature.

Case	Sex[a]/Age (year)	Underlying medical conditions	Clinical syndrome	Site of isolation	Treatment	Outcome	Reference
1	F/34	Chronic dermatomycosis	Granulomatous breast parenchymal lesions and cerebritis	Brain abscess	Patient refused treatment for underlying skin infection, treatment for the breast lesions and cerebritis was not mentioned	Died	[14,15]
2	M/70	Phacoemulsification and intraocular lens implantation	Wound infiltrate and abscess in the eye and subsequently impending corneal perforation	Surgical specimen of the eye	Oral ketoconazole (200 mg) with topical steroids added after 5 days; corneal transplantation, removal of superior iris, ciliary body and adjacent necrotic sclera in response to impending corneal perforation	Clinical remission	[20]
3	M/59	Coronary artery bypass surgery	Severe aortic regurgitation and congestive heart failure	Aortic valve	Aortic valve replacement with amphotericin B	Died on day 49 post operation	[17]
4	M/18	AIDS[b]	Fungaemia	Venous blood	Fluconazole (200 mg daily) for seven months	Clinical remission	[12]
5	M/44	Juvenile rheumatoid arthritis with methotrexate & prednisone therapy; and replacement of mitral valve & vegetation debridement, excision of the posterior cusp & cords, and annuloplasty of tricuspid valve due to previous endocarditis	Infective endocarditis	Bioprosthetic valve vegetation	Bioprosthetic valve replacement; parenteral liposomal amphotericin B (250 mg daily) and oral flucytosine (170 mg 4 times daily), and subsequently parenteral voriconazole (280 mg twice daily); oral voriconaole (200 mg twice daily) after discharge	Clinical remission	[18]
6	M/70	Trauma with vegetative matter at the right eye	Hypopyon corneal ulcer with endophthalmitis	Corneal scrapping	Oral fluconazole (150 mg twice daily); penetrating keratoplasty after 7 days	Clinical remission	[19]
7	M/60	Renal transplantation for end-stage renal failure with prednisolone, tacrolimus & azathioprine immunosuppressant therapy, recurrent urinary tract infections, cytomegalovirus reactivation and herpes zoster, as well as nontyphoidal *Salmonella* mycotic aneurysm at the infra-renal abdominal aorta	Crusted, non-tender lesion with overlying inflammatory skin changes at the right shin	Skin biopsy	Oral itraconazole (200 mg twice daily)	Died two months later due to nosocomial pneumonia with acute respiratory failure	This study

[a]F, female; M, male.
[b]AIDS, acquired immune deficiency syndrome.

In vitro antifungal susceptibility test suggested that posaconazole and voriconazole may be better choices when treating infection caused by *P. album*, while fluconazole and flucytosine should be avoided. Although all the clinical *P. album* isolates characterised in this study possessed high MICs (4 to >256 μg/ml) for fluconazole (Table 2), in a previous case of fungaemia[12] and a case of keratitis,[19] the patients recovered after receiving treatment with fluconazole. This showed that more clinical data have to be obtained before any correlation between the *in vitro* susceptibility data for fluconazole and clinical outcome could be established. As for posaconazole and voriconazole, most clinical *P. album* isolates, especially those belonging to subclades 2 and 3, had low MICs ($\leq$1 μg/ml) (Table 2), indicating these two antifungal agents may be the drugs of choice for the treatment of *P. album* infections. On the other hand, the use of itraconazole should be cautioned because its antifungal activity was totally different against strains belonging to subclade 1 (high MICs) and strains belonging to subclades 2 and 3 (low MICs) of *P. album* (Table 2). Unfortunately, for the present case the patient was treated with itraconazole before the susceptibility results were obtained, and he finally succumbed due to nosocomial pneumonia with acute respiratory failure. This highlighted the clinical importance of accurate identification of *P. album* strains down to the level of cryptic taxa since the antifungal susceptibility patterns differ among the different subclades.

DNA sequencing is by far the most reliable way to distinguish between *P. album* and other morphologically similar fungi. As revealed in the molecular analyses of this study, all the three DNA loci characterised, including the ITS, 28S nrDNA, and β-tubulin gene, are good DNA markers for identification. In addition, the ITS and β-tubulin gene could be used to identify *P. album* strains down to the level of cryptic taxa (Suppl. Fig. S1). As for the potential use of MALDI-TOF MS for *P. album* identification, although none of the fungal strains characterised in this study could be identified, HCA of the protein mass spectra of these fungal strains showed that genetically similar strains possessed similar MALDI-TOF protein mass spectra also (Fig. 6). Therefore, theoretically if sufficient protein mass spectra of the three subclades of *P. album* are included in the MALDI-TOF MS database and if the database is up-to-date, *P. album* isolates could be identified down to the level of cryptic taxa using MALDI-TOF MS.

Acknowledgements

This work is partly supported by the Strategic Research Theme Fund, Mary Sun Medical Scholarship, Wong Ching Yee Medical Postgraduate Scholarship, and University Postgraduate Scholarship, the University of Hong Kong, Hong Kong; and the Croucher Senior Medical Research Fellowship, Croucher Foundation, Hong Kong.

The authors are grateful to NRRL for providing the reference strain NRRL 2312 for free. The authors would also like to thank Ms Tonja Weilerscheid-Fung, School of Modern Languages and Cultures, the University of Hong Kong, Hong Kong, for her generous help in German translation.

Declaration of interest

Patrick C. Y. Woo has provided scientific advisory/laboratory services for Gilead Sciences Corporation and International Health Management Associates Corporation/Pfizer Corporation. Jasper F. W. Chan has provided scientific advisory services for Gilead Sciences Corporation, and received travel grants from Pfizer Corporation and Astellas Pharma Corporation. The other authors report no conflicts of interest. The funding sources had no role in study design, data collection, analysis, interpretation, or writing of the report. The authors alone are responsible for the content and the writing of the manuscript.

Supplementary Material

Supplementary material is available at *Medical Mycology* online (http://www.mmy.oxfordjournals.org/).

References

1. de Hoog GS. Notes on some fungicolous hyphomycetes and their relatives. *Persoonia* 1978; **10**: 33–81.
2. Gams W, de Hoog GS, Samson RA et al. The hyphomycete genus *Engyodontium*: a link between *Verticillium* and *Aphanocladium*. *Persoonia* 1984; **12**: 135–147.
3. Zare R, Gams W. A revision of *Verticillium* section Prostrata. IV. The genera *Lecanicillium* and *Simplicillium* gen. nov.). *Nova Hedwigia* 2001; **73**: 1–50.
4. Suresh PV, Chandrasekaran M. Impact of process parameters on chitinase production by an alkalophilic marine *Beauveria bassiana* in solid state fermentation. *Process Biochem* 1999; **34**: 257–267.
5. Chellappan S, Jasmin C, Basheer SM et al. Production, purification and partial characterization of a novel protease from marine *Engyodontium album* BTMFS10 under solid state fermentation. *Process Biochem* 2006; **41**: 956–961.
6. Yao Q, Wang J, Zhang X et al. Cytotoxic polyketides from the deep-sea-derived fungus *Engyodontium album* DFFSCS021. *Marine Drugs* 2014; **12**: 5902.
7. Wu H, Yang H-Y, You X-L et al. Diversity of endophytic fungi from roots of *Panax ginseng* and their saponin yield capacities. *SpringerPlus* 2013; **2**: 1–9.
8. Kachuei R, Emami M, Naeimi B et al. Isolation of keratinophilic fungi from soil in Isfahan province, Iran. *J Med Mycol* 2012; **22**: 8–13.
9. Jeffries P. Growth of *Beauveria alba* on mural paintings in Canterbury Cathedral. *Int Biodeterior* 1986; **22**: 11–13.
10. Simonovicova A, Godyova M, Kunert J. *Engyodontium album*, a new species of microscopic fungi for Slovakia and its keratinolytic activity. *Biologia, Bratislava* 2004; **59**: 17–18.

11. Ebeling W, Hennrich N, Klockow M et al. Proteinase K from *Tritirachium album* Limber. *Eur J Biochem* 1974; **47**: 91–97.
12. Macêdo DPC, Neves RP, Souza-Motta CMd et al. *Engyodontium album* fungaemia: the first reported case. *Braz J Microbiol* 2007; **38**: 110–112.
13. Kim HS, Park IY, Park YJ et al. A novel dihydroxanthenone, AGI-B4 with inhibition of VEGF-induced endothelial cell growth. *J Antibiot (Tokyo)*. 2002; **55**: 669–672.
14. Huhn FO, Stock G. Bericht über eine Fadenpilz-Granulomatose der Mamma als differentialdiagnostischer Beitrag zum Bild eines "inflammatorischen Karzinoms". *Geburtshilfe Frauenheilkd* 1977; **37**: 692–697.
15. Seeliger HPR. Infections of man by opportunistic molds—their identification and nomenclature of their diseases. *Mycoses* 1983; **26**: 587–598.
16. de Hoog GS. The genera *Beauveria*, *Isaria*, *Tritirachium* and *Acrodontium* gen. nov. *Stud Mycol* 1972; **1**: 1–41.
17. Augustinsky J, Kammeyer P, Husain A et al. *Engyodontium album* endocarditis. *J Clin Microbiol* 1990; **28**: 1479–1481.
18. Balasingham S, Chalkias S, Balasingham A et al. A case of bovine valve endocarditis caused by *Engyodontium album*. *Med Mycol* 2011; **49**: 430–434.
19. Thamke D, Mendiratta D, Dhabarde A et al. Mycotic keratitis due to *Engyodontium album*: first case report from India. *Indian J Med Microbiol* 2015; **33**: 303–304.
20. McDonnell PJ, Werblin TP, Sigler L et al. Mycotic keratitis due to *Beauveria alba*. *Cornea* 1984; **3**: 213–216.
21. Martynenko SV, Kondratyuk TO, Sukhomlin MM. A hyphomycete, *Engyodontium album* (Limber) de Hoog, attacking spiders in underground headings of Kyiv-city. *Ukr Botan J* 2012; **69**: 423–432.
22. Samson RA, Visagie CM, Houbraken J et al. Phylogeny, identification and nomenclature of the genus *Aspergillus*. *Stud Mycol* 2014; **78**: 141–173.
23. Woo PCY, Ngan AHY, Chui H-K et al. Agar block smear preparation: a novel method of slide preparation for preservation of native fungal structures for microscopic examination and long-term storage. *J Clin Microbiol* 2010; **48**: 3053–3061.
24. Tsang C-C, Hui TWS, Lee K-C et al. Genetic diversity of *Aspergillus* species isolated from onychomycosis and *Aspergillus hongkongensis* sp. nov., with implications to antifungal susceptibility testing. *Diagn Microbiol Infect Dis* 2016; **84**: 125–134.
25. Woo PCY, Ngan AHY, Tsang CCC et al. Clinical spectrum of *Exophiala* infections and a novel *Exophiala* species, *Exophiala hongkongensis*. *J Clin Microbiol* 2013; **51**: 260–267.
26. White T, Bruns T, Lee S et al. Amplification and direct sequencing of fungal ribosomal RNA genes for phylogenetics. In: Innis M, Gelfand D, Shinsky J et al., eds. *PCR Protocols: A Guide to Methods and Applications*. San Diego: Academic Press; 1990: 315–322.
27. O'Donnell K. *Fusarium* and its near relatives. In: Reynolds DR, Taylor JW, eds. *The Fungal Holomorph: Mitotic, Meiotic and Pleomorphic Speciation in Fungal Systematics*. Wallingford, UK: CAB International; 1993: 225–233.
28. Glass NL, Donaldson GC. Development of primer sets designed for use with the PCR to amplify conserved genes from filamentous ascomycetes. *Appl Environ Microbiol* 1995; **61**: 1323–1330.
29. Hall TA. BioEdit: a user-friendly biological sequence alignment editor and analysis program for Windows 95/98/NT. *Nucleic Acids Symp Ser* 1999; **41**: 95–98.
30. Edgar RC. MUSCLE: multiple sequence alignment with high accuracy and high throughput. *Nucleic Acids Res* 2004; **32**: 1792–1797.
31. Castresana J. Selection of conserved blocks from multiple alignments for their use in phylogenetic analysis. *Mol Biol Evol* 2000; **17**: 540–552.
32. Talavera G, Castresana J. Improvement of phylogenies after removing divergent and ambiguously aligned blocks from protein sequence alignments. *Syst Biol* 2007; **56**: 564–577.
33. Tamura K, Stecher G, Peterson D et al. MEGA6: Molecular Evolutionary Genetics Analysis version 6.0. *Mol Biol Evol* 2013; **30**: 2725–2729.
34. Sung G-H, Hywel-Jones NL, Sung J-M et al. Phylogenetic classification of *Cordyceps* and the clavicipitaceous fungi. *Stud Mycol* 2007; **57**: 5–59.
35. Tsang C-C, Chan JFW, Trendell-Smith NJ et al. Subcutaneous phaeohyphomycosis in a patient with IgG4-related sclerosing disease caused by a novel ascomycete, *Hongkongmyces pedis* gen. et sp. nov.: first report of human infection associated with the family *Lindgomycetaceae*. *Med Mycol* 2014; **52**: 736–747.
36. Irinyi L, Serena C, Garcia-Hermoso D et al. International Society of Human and Animal Mycology (ISHAM)-ITS reference DNA barcoding database—the quality controlled standard tool for routine identification of human and animal pathogenic fungi. *Med Mycol* 2015; **53**: 313–337.
37. Limber DP. A new form genus of the *Moniliaceae*. *Mycologia* 1940; **32**: 23–30.
38. Matsushima T. *Icones Microfungorum a Matsushima Lectorum*. Kobe: Matsushima; 1975.
39. de Hoog GS, Guarro J, Gené J et al. *Atlas of Clinical Fungi*, 2nd edn. Utrecht: Centraalbureau voor Schimmelcultures; 2000.
40. Tsang C-C, Chan JFW, Ip PPC et al. Subcutaneous phaeohyphomycotic nodule due to *Phialemoniopsis hongkongensis* sp. nov. *J Clin Microbiol* 2014; **52**: 3280–3289.
41. Hubka V, Dobiasova S, Lyskova P et al. *Auxarthron ostraviense* sp. nov., and *A. umbrinum* associated with non-dermatophytic onychomycosis. *Med Mycol* 2013; **51**: 614–624.
42. Hubka V, Dobiášová S, Dobiáš R et al. *Microsporum aenigmaticum* sp. nov. from *M. gypseum* complex, isolated as a cause of tinea corporis. *Med Mycol* 2014; **52**: 387–396.
43. Brasch J, Gräser Y. *Trichophyton eboreum* sp. nov. isolated from human skin. *J Clin Microbiol* 2005; **43**: 5230–5237.
44. Brasch J, Gräser Y. *Trichophyton eboreum* – a recently described dermatophyte. *J Dtsch Dermatol Ges* 2006; **4**: 646–649.
45. Keller MC, French LE, Hofbauer GFL et al. Erythematous skin macules with isolation of *Trichophyton eboreum* – infection or colonisation? *Mycoses* 2013; **56**: 373–375.